Mode Structure and Adaptive Control of the Jet-Edge-Flow

Arno Ickler, Dirk Ronneberger

Drittes Physikalisches Institut, D-37037 Göttingen, Germany, Email: Arno.Ickler@phsik3.gwdg.de

Introduction

The stabilisation of the plane laminar jet-edge-flow is studied with the general objective to gain experience in flow control. The convective instability of the jet combined with the feedback of pressure oscillations from the edge to the nozzle results in a global instability, which may evolve into a strong noise source. A feedback control system shall be added such that the flow becomes stable. The differences between this system and most mechanical and electrical feedback systems are the inherently high number of degrees of freedom and the imposibillity to realize an equivalent open loop system. The identification of the relevant system dynamics is done by an adaptive controller, which needs a small broad-band test-signal, in order to build a stabilising filter. For small distances between the nozzle and the edge a good stabilisation is achieved. However, the system becomes more sensitive to the parameters of the controller, when this distance is increased. Hence, and due to slow flow fluctuations of flow parameters, the adaption of the feedback filter must be done more carefully. Finally, at a certain distance the stabilisation fails. Furthermore, a robust adaptive control scheme and a comprehensive model of the flow shall be developed.

Experimental Setup

A plane laminar water jet (nozzle width $w=4\,\text{mm}$, jet velocity $u \approx 50\,\text{mm/s}$) impinges on the edge of a wedge, and the distance between the nozzle and the edge can be varied (figure 1); the jet oscillates at $1\,\text{Hz}$, typically. The
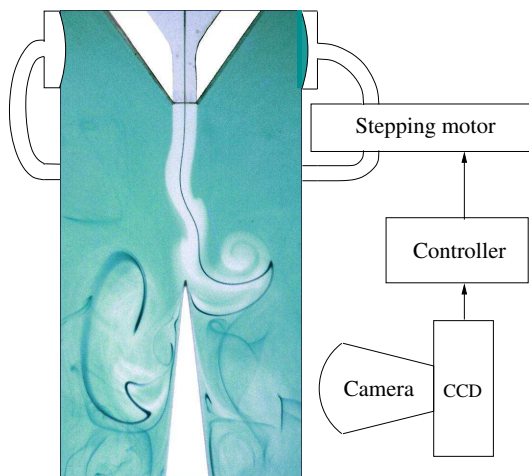

Figure 1: experimental setup of the jet-edge-system

central streakline of the jet is visualized by dye. So the lateral deflection of the jet can be measured at a fairly high accuracy ($0.01\,\text{mm}$, $0.02\,\text{s}$) by means of a CCD cam-

era and a real time image processing system. Two membranes are installed on both sides of the nozzle. They move in parallel in order to impose an antisymmetric pressure field on the flow which eventually shall compensate the pressure gradient at the nozzle.

Modes and their Dynamics

The jet oscillates at different modes (e.g. mode II in figure 1) characterized by the number of wavelengths between nozzle and edge, and depending on the jet edge distance. At certain distances the jet may oscillate at different modes with non harmonic frequency ratios. The red curve (mode II) in figure 2a is the power spectrum of the jet deflection (measured at a certain upstream position) with a frequency ratio $f_{\text{high}}/f_{\text{low}} = 2.8 \neq 3$ between the main peak frequencies, while the blue curve is a single mode oscillation with harmonics in the power spectrum. So the question arises whether mode II is a mixture of two modes or one self-contained mode. In the latter case a strong coupling of the 'incommensurable' frequency peaks is expected, which is not obvious. Describing the dynamics of the mode it is convenient to
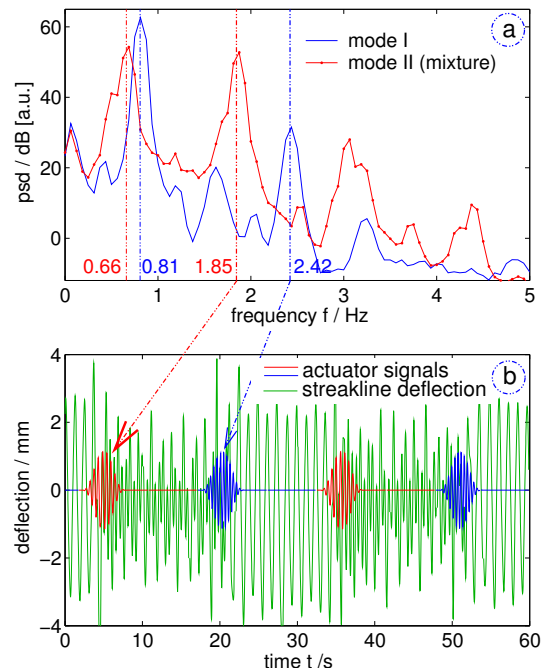
Figure 2: hysteresis and mode switching. a: power spectral density of the measured lateral streakline position, for mode I and mode II: nozzle-edge-distance 7 nozzle widths, $Re_w = 200$ b: a small actuator impuls with frequency of the second harmonic switches the native modes of the system

use the spatial mode characteristic to highlight the time development of the system. Using a proper orthogonal

decomposition, pairs of real eigen-functions can be combined to complex eigen-functions, considering the wave-like character of the instability. (Thus there is no need of short time spectral analysis.) In figure 3 the state of the system changes spontaneously from mode I to mode II (here $f_{\text{high}}/f_{\text{low}} = 2.95$). The obtained complex projection coefficients η represent the time development of the spatial characteristics corresponding to the frequency peaks. In average the phase $arg(\eta_{\text{high}})$ runs $f_{\text{high}}/f_{\text{low}}$ times faster then $arg(\eta_{\text{low}})$. However the phase-shift is not continously but rather in steps. Actually, the phase of the low frequency peak is triggered by the high, but if the phase exceeds a certain treshold, the system locks to the next stable phase relation. Imposing a short small
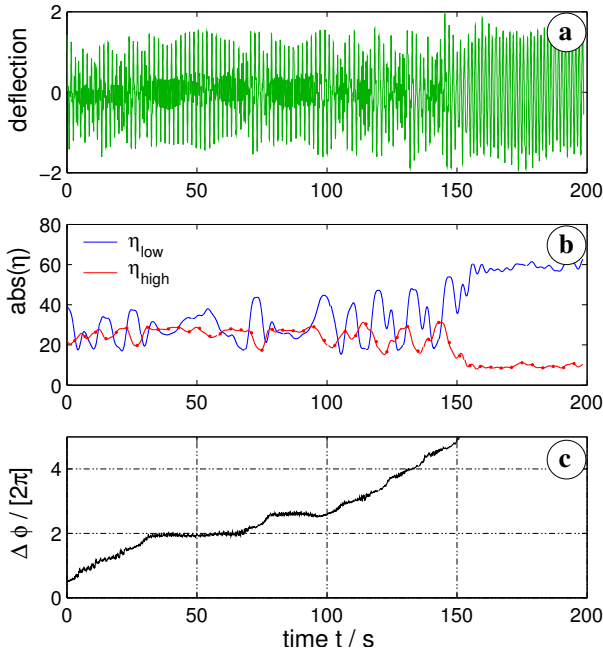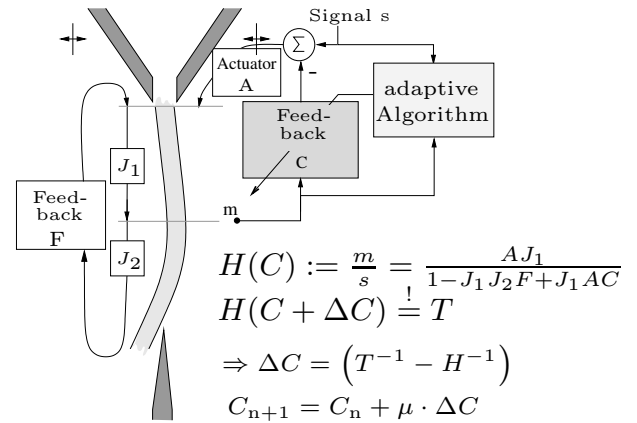

Figure 3: Natural mode II switching to mode I without control a: time series b: magnitude of the projection coeffiecent of the eigen-function representing the low/high frequency parts of the spectra c: $\arg(\eta_{\text{low}}) - \arg(\eta_{\text{high}})/3$

actuator signal with a frequency equal to the second 'harmonic' of the natural modes, the system synchronises its states. The time-series in figure 2b shows this forced mode switching. Keeping this fact in mind one has to handle this system very gently.

Adaptive Control

The model of the flow and the control scheme are depicted in figure 4: The dynamics of the jet including the convective amplification of disturbances is modelled by two linear transfer-functions J_1 and $J_1 \cdot J_2$ describing some lateral deflection of the jet that is introduced at the nozzle and is propagated to the measuring position and to the edge of the wedge, respectively. The unknown feedback $F \cdot J_2$ has to be canceled by the adaptive controller. The target transfer-function T (representing the estimated minimal correlation between the test-signal s and the measurement signal m) is obtained through a measurement without wedge. Choosing a suitable target

transfer-function, the adaptive algorithm is stable and the controller feedback C can be causally adapted. This

$$H(C) := \frac{m}{s} = \frac{A J_1}{1 - J_1 J_2 F + J_1 A C}$$
$$H(C + \Delta C) \overset{!}{=} T$$
$$\Rightarrow \Delta C = \left(T^{-1} - H^{-1}\right)$$
$$C_{\text{n}+1} = C_{\text{n}} + \mu \cdot \Delta C$$

Figure 4: adaptive control cheme

leads to a stabilisation of the flow up to a nozzle edge distance of 8 nozzle widths. The power spectral density of the measurement signal with and without control is depicted in Figure 5. The spectra indicates a mode mixture (b) so suppression is more complicate and the adaption must be more robust in presence of the fluctuations and the peak locking of the measurement system.

The estimated feedback C can then be used to obtain
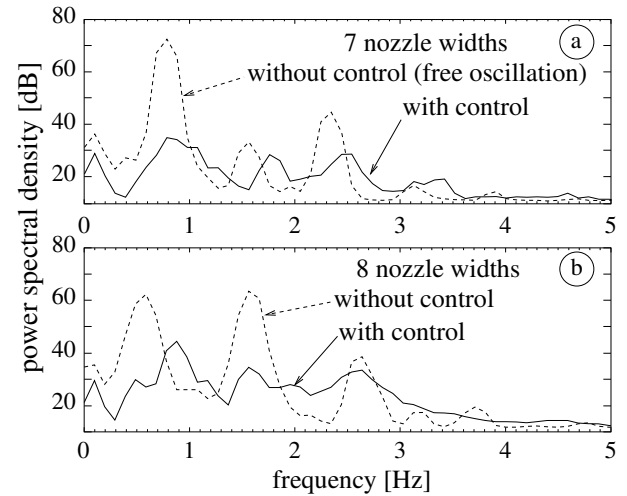
Figure 5: power spectral density of the measurement signal; with and without control for different nozzle egde distancies, Reynoldsnumber $U w/\nu \approx 200$ with nozzle width

an estimated physical feedback $F = \widehat{A} \cdot C \cdot \widehat{J_2^{-1}}$ from the wedge to the nozzle. So a physical model of F can be developed.

References

[1] Preckel, H.: *Dynamik und Steuerung der Strahl-Kanten-Strömung*, Diss. Math.-Nat. Fak. Univ. Göttingen (1999)

[2] movies of stabilization. URL: `http://www.physik3.gwdg.de/~arno`